First-passage percolation under extreme disorder: From bond percolation to Kardar-Parisi-Zhang universality

Daniel Villarrubia,[1] Iván Álvarez Domenech,[1] Silvia N. Santalla,[2] Javier Rodríguez-Laguna,[3] and Pedro Córdoba-Torres[1,*]
[1]*Dpto. Física Matemática y de Fluidos, UNED, Spain*
[2]*Dpto. Física & GISC, Universidad Carlos III de Madrid, Spain*
[3]*Dpto. Física Fundamental, UNED, Spain*

(Received 19 December 2019; revised manuscript received 1 April 2020; accepted 12 May 2020; published 16 June 2020)

We consider the statistical properties of arrival times and balls on first-passage percolation (FPP) two-dimensional square lattices with strong disorder in the link times. A previous work showed a crossover in the weak disorder regime, between Gaussian and Kardar-Parisi-Zhang (KPZ) universality, with the crossover length decreasing as the noise amplitude grows. On the other hand, this work presents a very different behavior in the strong-disorder regime. An alternative crossover length appears below which the model is described by bond-percolation universality class. This characteristic length scale grows with the noise amplitude and diverges at the infinite-disorder limit. We provide a thorough characterization of the bond-percolation phase, reproducing its associated critical exponents through a careful scaling analysis of the balls, which is carried out through a continuous mapping of the FPP passage time into the occupation probability of the bond-percolation problem. Moreover, the crossover length can be explained merely in terms of properties of the link-time distribution. The interplay between the characteristic length and the correlation length intrinsic to bond percolation determines the crossover between the initial percolation-like growth and the asymptotic KPZ scaling.

DOI: 10.1103/PhysRevE.101.062124

I. INTRODUCTION

Geometry on random manifolds presents both applied and fundamental interest, with applications ranging from the physics of polymers and membranes [1,2] to quantum gravity [3–5]. Specifically, *geodesics* and *isochrones* on random manifolds, corresponding to non-Euclidean versions of straight lines and circumferences, present a very rich behavior [6,7]. It was recently shown that, in the case of random surfaces which are flat on average and with short-range correlations in the curvature, geodesics present fractal structure, governed by exponents corresponding to the celebrated Kardar-Parisi-Zhang (KPZ) universality class [8] describing random interfacial growth [9–12]. Specifically, the lateral deviation of a geodesic joining two points separated an Euclidean distance L scales like $L^{1/z}$, where $z = 3/2$ is the dynamical exponent of KPZ. Moreover, the deviation of the arrival times scales like L^{β}, with $\beta = 1/3$, and their fluctuations follow the Tracy-Widom distribution for the lowest eigenvalues of random unitary matrices [13–15].

When the manifold is discretized the problem is called *first-passage percolation* (FPP) [16–18]. Given an undirected lattice, e.g., $\mathbb{Z}^2$, a randomly chosen link time t is assigned to each edge between neighboring nodes. Link times are independent and identically distributed random variables with common probability density function $f(t)$ and cumulative distribution function $F(t)$. Notice that for the model to present the structure of a metric space we must assume $F(0) = 0$. This problem bears a strong relation with the *directed polymers in random media* (DPRM) [19–21], where we study the free-energy fluctuations of a polymer on a random surface. FPP results have been successfully applied to magnetism [22], wireless communications [23], ecological competition [24], and molecular biology [25].

The main objects of study in FPP are geodesics, i.e., minimal time paths joining pairs of points, and balls $B(T)$ given by the set of nodes which can be reached from the origin in a time less than T. There are some rigorously proved results, such as the *Galilean invariance*, $z(1 + \beta) = 2$ [26]. A *shape theorem* has been proven [27–29], stating that when the lattice structure is properly smoothed out, the ball $B(T)$ grows linearly with T and has an asymptotic shape B_0 which is nonrandom. Moreover, for suitable conditions on the moments of F, B_0 is a convex set with nonempty interior, and it is either compact or equals all of $\mathbb{R}^d$ [29].

In a previous work [30] we showed that FPP presents alternative features over the continuous version of the problem in the weak disordered regime. For weakly *degenerated* lattice directions (which can be found in both regular and disordered lattices), KPZ universality appeared beyond a characteristic length, $d_c \sim (\tau/s)^2$, where τ and s are, respectively, the mean value and standard deviation of the link times.

Yet, for a strong noise, i.e., $s \gg \tau$, the characteristic length $d_c < 1$ cannot play the same role. In some relevant cases, s and τ might even be ill-defined. Indeed, in the *strong-disorder regime*, link times encompass several orders of magnitude. A limit case is given by the Bernoulli distribution, in which link

*Corresponding author: pcordoba@dfmf.uned.es

times can be zero with probability $p = F(0)$. If we identify now zero-time links with open bonds in a connected lattice, we are effectively mapping our system to a problem of *bond percolation* [21,29,31]. Thus we have *critical FPP* defined by condition $F(0) = p_c$ [32–36] and *supercritical FPP* defined by $F(0) > p_c$ [37–39], where p_c is the critical probability in bond percolation [31]. For $F(0) \geqslant p_c$ there exists an infinite connected set of edges with zero crossing time so that traveling across this infinite cluster costs no time [40]. As a consequence, the *route* between two lattice nodes will always stay within the infinite cluster except for a few edges [37]. Furthermore, it has been shown that the asymptotic shape B_0 equals all of $\mathbb{R}^d$ if and only if $F(0) \geqslant p_c$ [41,42].

Much effort in critical FPP has been devoted to the analytical study of the *time constant* μ, defined as the limit of the passage time to a site (or to some boundary) normalized by its distance from the origin, as the distance goes to infinity. This limit has been proven to exist for suitable conditions on the moments of F [43], and $\mu = 0$ if and only if $F(0) \geqslant p_c$ [29]. Indeed, the existence of large clusters with zero-time edges leads to a passage time that grows at most logarithmically with distance, yielding a zero-time constant [32,33,35]. Previous work has focused on the characterization of the asymptotics of this arrival time by conditions on the distribution function F [32–36], yielding relevant results such as a universal expression for the time constant on two-dimensional lattices [33], the proposition of a central limit theorem for the passage time [35,36], or a relation between critical FPP and invasion percolation [32].

The geometry of the minimal paths has also been a matter of study [44]. In the early 1980s, Ritzenberg and Cohen considered shortest paths on a *percolation cluster* beyond criticality, i.e., spanning an infinite number of nodes [45], computing their fractal dimension. Kerstein and coworkers considered FPP with two possible link times, a slow one and a (extremely) fast one [46–48]. They describe, as the density of slow links increases, a crossover from *chemical* to *contact propagation*. Chemical propagation describes geodesics that employ only fast links, while contact propagation refers to the use of slow links to jump from cluster to cluster. In the first case, the conduction rate is limited by the geodesic *tortuosity*, i.e., the average number of links along a typical fast path. For contact propagation, on the other hand, the conduction rate is limited by the ratio of slow bonds. The crossover between both regimes takes place at the percolation threshold. Geodesics on critical and supercritical percolation clusters were studied by several authors [32,35,37–39,49], and a correspondence between geodesics on critical percolation clusters and Schramm-Loewner evolution curves has been recently put forward [50], lending support to the idea that they might be conformally invariant [51].

In this article, we characterize the statistical properties of arrival times and balls on strongly disordered networks. Our purpose is to study the behavior of the model close to the critical case discussed so far, but keeping the condition $F(0) = 0$ that is necessary for it to represent a metric space. We propose a mapping of the passage time into the probability p of a bond being open, which allows us to map the FPP problem into a family of bond-percolation problems. Making use of detailed numerical simulations, we show how the scaling exponents of percolation theory map into those of the geodesic behavior below a certain crossover length, above which the geodesics attain the standard KPZ behavior. This crossover length increases with the noise amplitude and seems to diverge for infinite noise, which leads us to conjecture that this limit might be related to the critical or supercritical FPP cases, depending on the link-time distribution.

This article is organized as follows. Section II presents the first-passage percolation model and our basic assumptions. Next, in Sec. III we compare the statistical properties of the arrival times in the weak and strong disorder regimes. The mapping of the FPP problem into bond percolation is addressed in Sec. IV, where we also present a comprehensive scaling analysis of the FPP balls that recovers the critical exponents of percolation. In Sec. V we propose a model for the characteristic length that controls the extent of the percolation domain. Large-scale behavior and the crossover towards standard KPZ scaling is described in Sec. VI, in which we also discuss the transition between the weak and strong disorder regimes. Section VII is devoted to a summary of our conclusions and our ideas regarding future work.

II. MODEL AND DEFINITIONS

Let us consider a $L \times L$ square lattice (odd L), with nodes $\mathbf{x}_i$ and a central node $\mathbf{x}_0 = (0, 0)$. We assign a link time $t(\mathbf{x}_i, \mathbf{x}_j)$ to each pair of nearest-neighbor nodes, $\mathbf{x}_i$ and $\mathbf{x}_j$. Given a path $\Gamma = \{\mathbf{x}_0, \mathbf{x}_1, \ldots, \mathbf{x}_m\}$ joining the center to site $\mathbf{x}_m$, in order to traverse that path we would need a time

$$T_\Gamma(\mathbf{x}_m) = \sum_{i=1}^{m} t(\mathbf{x}_{i-1}, \mathbf{x}_i). \tag{1}$$

We define the *arrival time* as the minimal value over all paths reaching arbitrary node $\mathbf{x}$ from $\mathbf{x}_0$:

$$T(\mathbf{x}) \equiv \min_\Gamma \{T_\Gamma(\mathbf{x})\}, \tag{2}$$

and the corresponding path is the *geodesic* or *optimal path* to that point. For a continuous distribution of link times the geodesic will be unique. Let us remark that arrival times can be efficiently obtained for all sites making use of *Dijkstra's algorithm* [52]. Finally, we also define the ball $B(T)$ as the set of nodes which can be reached in a time smaller than a certain value T.

We consider the case in which link times are independent and identically distributed random variables with common probability density function $f(t)$ and cumulative distribution function $F(t)$, with the only constraint of positivity: $F(0) = 0$. If they exist, the link-time distribution is characterized by a mean value τ and a variance s^2,

As discussed in the introduction, it has been shown that the appearance of KPZ universality for weak disorder is ruled by a direction-dependent crossover associated with the so-called *geodesic degeneracy*, i.e., the number and structure of the geodesics joining two points in the absence of noise [30]. Indeed, a characteristic length d_c was found both in the square lattice and in random Delaunay triangulations, determining a crossover between Gaussian and KPZ behavior. This crossover length can be conventionally defined as $d_c \equiv \tau^2/(3s^2) = (3\mathrm{CV}^2)^{-1}$, where the numerical factor 3 is inserted for later convenience and CV is the *coefficient of*

variation, $\mathrm{CV} = s/\tau$. Notice that d_c decreases as the noise increases. Arrival times to sites along the axis of a square lattice at a distance $x \ll d_c$ follow Gaussian statistics and KPZ statistics for $x \gg d_c$. Indeed, in that case the geodesic will not deviate from the straight line up to a distance $\sim d_c$. This behavior is expected to occur along nondegenerate directions of regular lattices and in low degenerated random lattices such as Delaunay triangulations. On the other hand, for disordered distributions with $\tau < s$ (CV > 1) thus giving $d_c < 1$ we enter the *strong disorder* regime, and the statistical properties of the arrival times change considerably.

Uniform link-time distributions have necessarily $d_c > 1$ (note that CV $< 3^{-1/2}$). Yet other distributions interpolate smoothly between these two regimes. We require link-time distributions to uphold the following properties: (a) the link times must be always positive and (b) the range of disorder must be large, i.e., for some range of the distribution parameters, the deviation must be larger than the average value. We have chosen three distributions fulfilling those requirements: Weibull, log-normal, and Pareto. They have been chosen because their mathematical expressions allow a simple analytic treatment. Furthermore, the strength of the disorder can be easily tuned through a single parameter, which is usually called the *shape parameter*. The mathematical expressions for the probability density function $f(t)$ and the cumulative distribution function $F(t)$ of those distributions are the following:

(i) The Weibull distribution, $\mathrm{Wei}(\lambda, k)$:

$$f(t) = \frac{k}{\lambda}\left(\frac{t}{\lambda}\right)^{k-1} \exp[-(t/\lambda)^k],$$
$$F(t) = 1 - \exp[-(t/\lambda)^k]. \tag{3}$$

The results displayed in this work do not depend on the scale parameter λ, so we have considered $\lambda = 1$ in all the numerical simulations. As we will see, it is the so-called *shape parameter* k which completely determines the strength of the disorder.

(ii) The log-normal distribution, $\mathrm{LogN}(\mu, \sigma)$:

$$f(t) = \frac{1}{t\sqrt{2\pi\sigma^2}} \exp\left[-\frac{(\ln t - \mu)^2}{2\sigma^2}\right],$$
$$F(t) = \frac{1}{2} + \frac{1}{2}\mathrm{erf}\left[\frac{\ln t - \mu}{\sqrt{2\sigma^2}}\right]. \tag{4}$$

The above comment about the parameters of the Weibull distribution also applies here to parameters μ and σ, respectively.

(iii) The Pareto distribution, $\mathrm{Par}(t_m, \alpha)$:

$$f(t) = \begin{cases} \frac{\alpha t_m^\alpha}{t^{\alpha+1}} & \text{if } t \geqslant t_m \\ 0 & \text{if } t < t_m \end{cases},$$
$$F(t) = \begin{cases} 1 - \left(\frac{t_m}{t}\right)^\alpha & \text{if } t \geqslant t_m \\ 0 & \text{if } t < t_m \end{cases}, \tag{5}$$

with the above remark applying to scale t_m and shape α parameters, respectively.

We will refer as the *homogenous case* to the case with no noise, i.e., when link times follow the δ distribution $f(t) = \delta(t - \tau_0)$ so they present a uniform value τ_0. The homogeneous case is obtained at the following limits of the above distributions:

$$\lim_{k\to\infty} \mathrm{Wei}(\lambda, k) = \delta(t - \lambda),$$
$$\lim_{\sigma\to 0} \mathrm{LogN}(\mu, \sigma) = \delta(t - e^\mu), \tag{6}$$
$$\lim_{\alpha\to\infty} \mathrm{Par}(t_m, \alpha) = \delta(t - t_m).$$

The value of d_c can be expressed in a closed form for all of them. For the Weibull distribution,

$$d_c(k) = \frac{1}{3}\frac{\Gamma^2\left[1 + \frac{1}{k}\right]}{\Gamma\left[1 + \frac{2}{k}\right] - \Gamma^2\left[1 + \frac{1}{k}\right]}, \tag{7}$$

and the crossover value of k for which $d_c = 1$, denoted here as $k^\star$, is

$$k^\star \equiv k(d_c = 1) \approx 1.79. \tag{8}$$

For the log-normal distribution we have

$$d_c(\sigma) = \frac{1}{3}\frac{1}{e^{\sigma^2} - 1} \quad \text{with} \quad \sigma^\star \approx 0.54, \tag{9}$$

and for Pareto

$$d_c(\alpha) = \frac{1}{3}\alpha(\alpha - 2) \quad \text{with} \quad \alpha^\star = 3. \tag{10}$$

Note that the last expression holds only for $\alpha > 2$ since the standard deviation s diverges when $\alpha \leqslant 2$ and the mean time τ diverges if $\alpha \leqslant 1$. For $\alpha \leqslant 2$ we shall assume that $d_c = 0$.

In all three cases d_c is a monotonic function of the shape parameter: it decreases and approaches 0 as the dispersion of the distribution increases ($k \to 0$, $\sigma \to \infty$ and $\alpha \to 0$) and diverges as the distributions approach the δ distribution ($k \to \infty$, $\sigma \to 0$ and $\alpha \to \infty$). In order to unify our description we introduce the concept of *order factor* to identify the distribution parameter which, when increasing, makes the strength of disorder decrease in a monotonic way. We thus identify k, σ^{-1} and α as the corresponding order factors of the above distributions. For the sake of clarity we will denote this order factor by ω. As a result of this convention, d_c is always an increasing monotonic function of ω, and the homogeneous case is obtained at the "infinite order" limit $\omega \to \infty$ of the distribution [see Eq. (6)]. Accordingly, the opposite limit $\omega \to 0$ will correspond to the limit of "infinite disorder." We also introduce the symbol $\omega^\star$ to denote the value of the order factor yielding $d_c = 1$: $d_c(\omega^\star) = 1$. In other words, $\omega^\star$ determines the crossover point between the weak ($\omega \gg \omega^\star$ and $d_c \gg 1$) and the strong ($\omega \ll \omega^\star$ and $d_c \ll 1$) disorder regimes. We will employ the term *order factor* and the symbol ω when we discuss generic properties which apply to all the considered distributions.

Before going in depth into the analysis of the model, it is worth having a look at the different behaviors at both sides of this divide. Figure 1(a) shows the FPP ball $B(T)$ obtained at $T = 25$ on a $L = 101$ lattice whose link-crossing times are drawn from a Weibull distribution with $\lambda = 1$ and $k = 2$, for which $d_c \approx 1.22$. The final ball appears *rough*, and indeed this roughness can be shown to correspond to the well-known KPZ universality class. Colors provide information about the arrival time to all sites within the ball, which we can see to behave in a reasonable smooth way. On the other hand, Fig. 1(b) corresponds to $T = 0.1$ for a distribution with

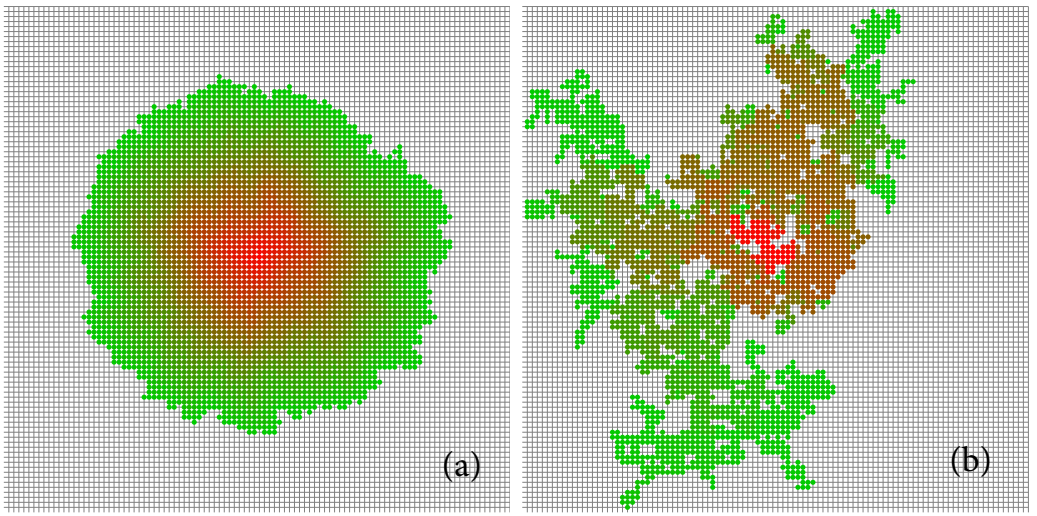

FIG. 1. (a) FPP ball corresponding to $T = 25$ on a square lattice, for a link-time Weibull distribution Wei(1,2). Colors are associated to different arrival times. (b) FPP ball corresponding to $T = 0.1$ when the link times are drawn from Wei(1,0.1). Notice that the crossover value of the order factor is $k^\star \approx 1.79$.

$\lambda = 1$ and $k = 0.1$, for which $d_c \approx 2 \times 10^{-6}$. Notice that the aspect of the ball is much less round, with abundance of *cavities*. Another salient feature is the *sharpness* of the color gradation. Instead of a smooth variation, we can determine clear boundaries within the ball.

III. FLUCTUATIONS OF THE ARRIVAL TIMES: FROM WEAK TO STRONG DISORDER

Let us explore numerically the statistical properties of the arrival times using a $L \times L = 2001 \times 2001$ lattice and link times drawn from the distributions presented above with different values of the order factor, in order to interpolate smoothly from the weak to the strong-disorder regimes. Moreover, we will always average over $N_s = 10^4$ samples, unless otherwise stated. As in Fig. 1, most of the results displayed hereafter will be obtained from the Weibull distribution, for which the crossover value of the order factor is $\omega^\star = k^\star = 1.79$. The simulations performed using the other distributions show that they behave in a similar manner. The very few cases where significant differences appear with respect to the Weibull distribution will be discussed. In addition, when necessary, results will be appropriately rescaled by statistical measures of the link-time distribution such as τ or s, so they will be independent of parameter λ, which will always be taken as 1.

Let us consider the average arrival time in units of the average link time, $\langle T \rangle / \tau$, for sites on the axis as a function of their Euclidean distance to the center, $x = \|\mathbf{x}\|$. In the weak disorder regime [30] this magnitude grows linearly with the distance for $x \gg d_c$, and the slope continuously decreases as the order factor decreases. This slope represents the inverse of the normalized velocity of growth and is closely related to the *time constant* μ discussed in the introduction. It is bounded from above by the trivial value obtained in the homogeneous case ($\omega \to \infty$): 1 in the axis and $\sqrt{2}$ for the diagonal, leading to balls with diamond shapes. As the order factor decreases, the slopes found in all lattice directions decrease (velocity increases), and when ω approaches the crossover value $\omega^\star$ ($d_c \to 1$), they become equal, thus explaining the circular shape of the balls in average [see, e.g., the ball shown in Fig. 1(a)].

Figure 2(a) shows $\langle T \rangle / \tau$ as a function of the distance x along the axis, when the link times follow the Weibull distribution with $k = 0.2$. The arrival time seems to approach a linear growth with distance, with a slope much smaller than one. For reasons that will become apparent soon, we have employed two different sample sizes: $N_s = 10^3$ (solid squares) and $N_s = 10^4$ (red open circles), which coincide perfectly. Figure 2(b) shows the values of $\langle T \rangle / \tau$ as a function of the distance x when the link times are drawn from a link-time distribution with a much lower value of the order factor $k = 0.03$, i.e., deep in the strong-disorder regime ($k \ll k^\star$). In this case, the times of arrival appear scattered, without a clear dependence on the distance. Moreover, the data for $N_s = 10^3$ (solid squares) and $N_s = 10^4$ (red open circles) are statistically different. This fact suggests that the arrival times in this regime are very difficult to sample, pointing to an extremely broad distribution.

To understand this behavior we have displayed in Fig. 3 the distribution of the arrival times to a given node $\mathbf{x}$, denoted by $g_{\mathbf{x}}(T)$. In Fig. 3(a) we have considered a fixed position along the axis, $x = 500$, and link-time distributions of the form Wei(1,k) for different values of k. Figure 3(b) displays the results for the strongly disordered case with $k = 0.03$ at different points along the axis.

In the weak-disorder regime, the distribution of arrival times at distance $x \gg d_c$ has been shown to follow the Tracy-Widom distribution for the Gaussian unitary ensemble (GUE) [13–15,30], which appears in Fig. 3(a) (case $k = 2$) in the form of a small and sharp peak (notice the log scale). However, as the disorder strength increases the distribution becomes right-skewed with the arrival time spanning an increasing range of orders of magnitude. The distribution still presents a well-defined mode that moves towards smaller values and that is followed by a increasingly longer

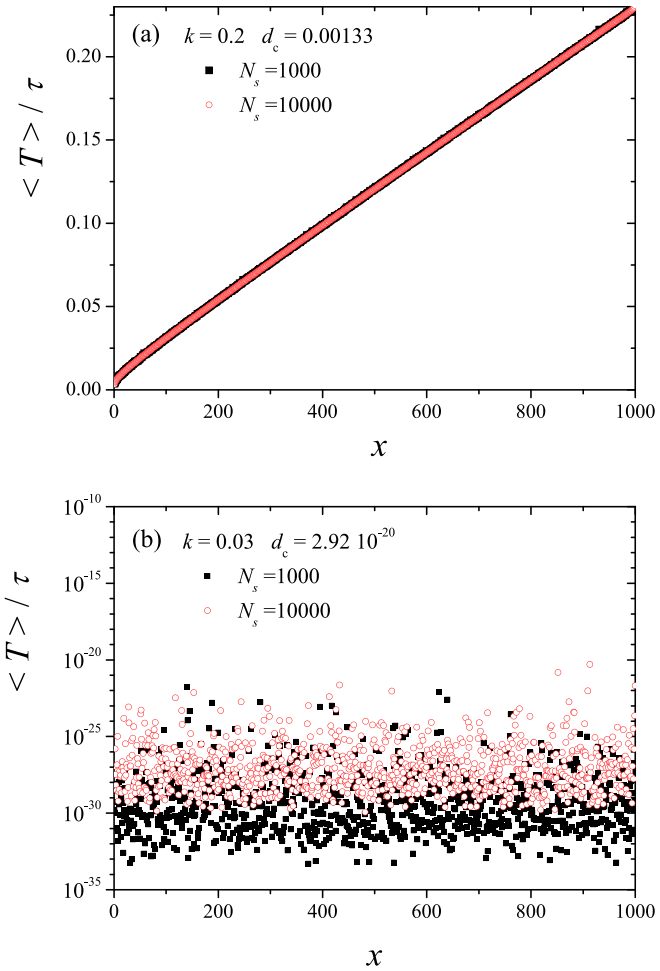

FIG. 2. Average passage time, rescaled to the mean link time τ, to nodes at a distance x along the axis for the Weibull distribution with $k = 0.2$ (a) and $k = 0.03$ (b). Results from two ensembles with $N_s = 1000$ and $N_s = 10\,000$ samples have been represented in both cases with black squares and red open circles, respectively.

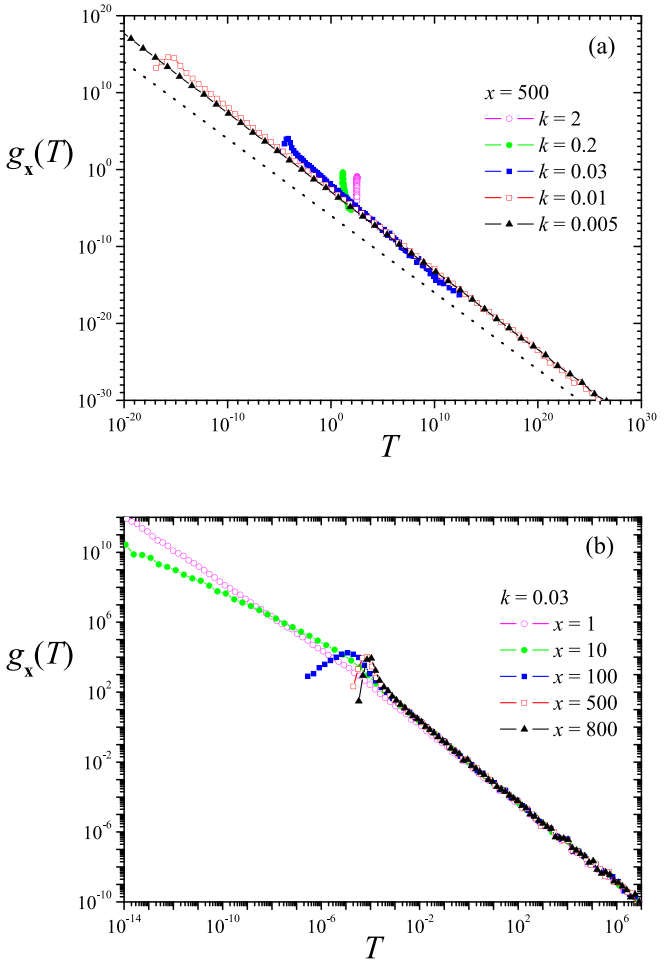

FIG. 3. Histogram of passage times T to (a) site at distance $x = 500$ along the axis for different values of k and (b) different sites along the axis for the same value of $k = 0.03$. The dotted line in panel (a) indicates the scaling $\sim T^{-1}$.

tail displaying a power-law scaling $\sim T^{-1}$ as $k \to 0$. As as consequence, for extreme disorder the mean arrival time is not well defined, and its average value is dominated by the largest value: $\langle T \rangle(\mathbf{x}) = \frac{1}{N} \sum_i^N T_i(\mathbf{x}) \simeq \frac{1}{N} T_{\max N}(\mathbf{x})$, where $T_{\max N}(\mathbf{x}) = \max_i\{T_i(\mathbf{x})\}$, which certainly depends on the sample size, thereby explaining the results displayed in Fig. 2(b).

Let us now focus on the dependence of the passage-time distribution on the distance for highly disperse distributions [case $k = 0.03$, Fig. 3(b)]. We observe that the right tails of the skewed distributions merge into a single decay regardless of the position of the target point. This result, together with the max principle stated above, explains the independence of the average time $\langle T \rangle$ with distance displayed in Fig. 2(b). Furthermore, as we move away from the center node, the distributions seem to approach a limit function, which suggests that the minimum arrival time required to reach any lattice site is independent of its position. The existence of such minimal arrival time is evidence of criticality in the model.

Another physical quantity of immediate interest in the study of the FPP model is the standard deviation of the arrival times. In the KPZ regime ($\omega \gg \omega^\star$ and for $x \gg d_c$) it scales as $\sigma_T \sim x^\beta$, with $\beta = 1/3$, following the Family-Vicsek ansatz. This standard deviation also corresponds to the roughness of the balls [6] and is analogous to the free energy fluctuations in directed polymers in random media (DPRM) [21].

In Fig. 4 we have plotted the standard deviation of the arrival time σ_T, in units of the deviation of the link-time distribution, s, to nodes on the axis as a function of their distance x to the center. In all cases we are employing the Weibull distribution Wei(1,k) for different values of k which have been indicated along with the corresponding d_c. For $k > k^\star$ ($k = 2$ up to $k = 30$) we observe the well-known crossover from Gaussian towards KPZ scaling, with a behavior $\sigma_T \sim x^{1/2}$ for $d \ll d_c$ and $\sigma_T \sim x^{1/3}$ for $d \gg d_c$ [30]. Moreover, for $x = 1$ we have $\sigma_T/s \approx 1$ because the geodesic from a site to its neighbor usually consists of traversing the link joining them. On the other hand, for $k < k^\star$ we observe that σ_T/s at $x = 1$ is always below 1, and it decreases very fast as $k \to 0$ implying that the geodesic between a site and its neighbor is certainly nontrivial. This fact suggests that geodesics in the strong-disorder regime can take long excursions in order to cover short distances on the lattice. Indeed, the geometric constraints imposed by the lattice are removed by the disorder,

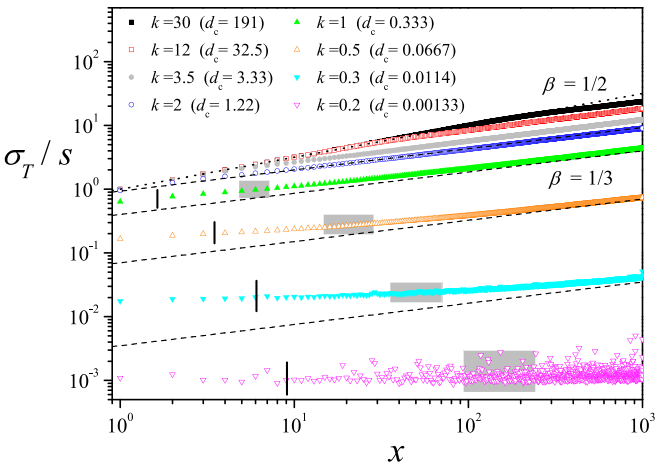

FIG. 4. Standard deviation σ_T of the arrival time to nodes at distance x in the axis of the square lattice with link times following a Wei(1,k) distribution, normalized to the standard deviation of the link-time distribution s. The corresponding values of d_c are calculated from Eq. (7). Dotted lines represent Gaussian preasymptotic growth ($\beta = 1/2$), and dashed lines denote KPZ scaling ($\beta = 1/3$). Vertical segments in curves with $d_c < 1$ ($k < k^\star$) indicate the value of length $\ell_k(T_c)$ obtained from the chain model presented in Sec. V. Gray rectangles represent the interval $[\ell_k(T(p = 0.99)), \ell_k(T(p = 0.999))]$, as discussed in Sec. VI.

and the geodesics are never constrained to follow the axis (such as in the Gaussian regime for $k > k^\star$ and $x \ll d_c$) and explore the space freely in any direction.

Moreover, Fig. 4 shows that below $k^\star$ there appears an increasingly long different pre-asymptotic regime along which fluctuations do not increase with distance. As indicated in the figure with the dashed lines, the KPZ regime $\sigma_T \sim x^{1/3}$ is always recovered for sufficiently large distances. Clearly the crossover point between both regimes increases as the order factor decreases. In the figure we have indicated with vertical segments and shadowed intervals theoretical estimates for the location of this crossover length according to the calculations that we present later. See Sec. VI for an explanation and discussion of these estimates.

A thorough explanation of the results presented in this section will be given in the following sections.

IV. MAPPING OF FPP UNDER EXTREME DISORDER INTO BOND PERCOLATION

Strongly disordered link-time distributions lead to an interesting phenomenon: the arrival time, which is by definition the sum of all link times along the geodesic path, is *dominated by its largest term*. Then we can assert that

$$T(\mathbf{x}) = \min_{\Gamma} \sum_{i=1}^{m} t(\mathbf{x}_{i-1}, \mathbf{x}_i) \approx \min_{\Gamma} \left\{ \max_{i} \{t(\mathbf{x}_{i-1}, \mathbf{x}_i)\} \right\}, \quad (11)$$

i.e., arrival times follow a min-max principle, for which we provide evidence in the Appendix. If this principle holds exactly, the set of points which can be reached in time T corresponds to the set of points for which there is a path which never crosses a link with crossing time larger than (or equal to) T. Moreover, the perimeter of the ball will be surrounded by links with crossing time $t \geqslant T$. Thus, a clear connection with percolation can be established: the FPP ball obtained at time T, $B(T)$, corresponds to the cluster obtained in an equivalent *bond percolation* problem in which open bonds correspond to those FPP links with crossing times lower than T, whereas closed bonds are given by the FPP links with crossing time above T. To establish this equivalence we need to define the probability p of a bond being open ($1 - p$ of being closed). Under the assumption made in Eq. (11) this probability is given by the cumulative distribution function of the link times evaluated at time T:

$$p = F(T) = \int_0^T f(t)\, dt. \quad (12)$$

This section is devoted to providing strong evidence that under extreme disorder conditions the FPP problem can be mapped into a bond-percolation problem through relation (12), which is the cornerstone of this work. Clearly the inverse transformation is given by $T = F^{-1}(p)$. For example, for the Weibull distribution we obtain

$$p(T) = 1 - \exp[-(T/\lambda)^k],$$
$$T(p) = \lambda[-\ln(1 - p)]^{1/k}. \quad (13)$$

Notice that $p(T)$ increases continuously with T, with $p(0) = 0$ and $p \to 1$ as $T \to \infty$. Also, the passage time corresponding to a given probability decreases monotonically as k decreases, approaching 0 as $k \to 0$.

We will show that FPP balls with arrival time T are equivalent to bond-percolation clusters obtained at bond probability $p = F(T)$. The mapping given in Eq. (12) will allow us to obtain some of the most relevant critical exponents of the associated percolation problem from the scaling analysis of the FPP geodesic balls. In the analysis we will use the standard notation of percolation theory [31]. Since we are interested in the strong disorder regime we have to consider very low values of the order factor $\omega \ll \omega^\star$. In the case of the Weibull distribution we shall focus on three values: $k = 0.03$, 0.01, and 0.005, because they are sufficiently low to display the transition to the percolation phase at a reasonable computational cost (we recall that $k^\star \approx 1.79$).

A. Ball size distribution

Percolation theory [31] deals primarily with the statistical properties of clusters of neighboring sites that are occupied (site percolation) or connected by open bonds (bond percolation), when each site (or bond) is occupied (open) with a probability p. The *critical point* or *percolation threshold* p_c is defined as the minimal probability p for which an infinite percolation cluster is formed in an infinite lattice. Near the critical point the system is characterized by a set of critical exponents that are independent of the type of percolation or the lattice geometry, and they depend only on the dimension D of the lattice. On the other hand, the percolation threshold varies with all these factors. For bond percolation in a $D = 2$ square lattice it is $p_c = 1/2$.

Let $n_s(p)$ be the number of clusters of size s (i.e., with s sites), divided by the total number of lattice sites. This observable is known to present the following scaling relation

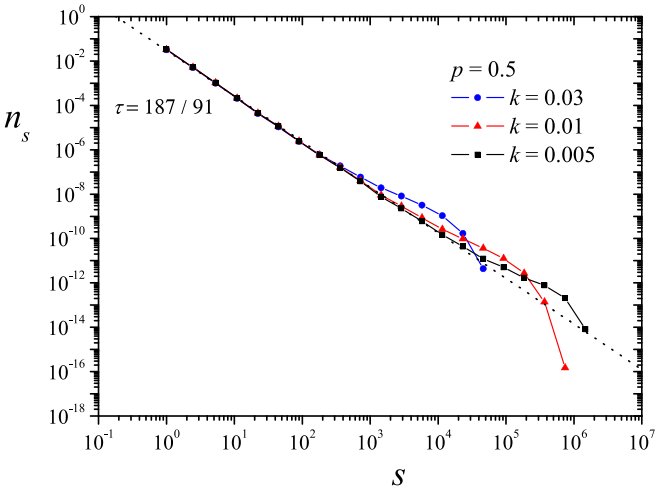

FIG. 5. Ball size distribution, derived from the probability W_s of obtaining a FPP ball with size s, using Eq. (16), for crossing times following a distribution Wei(1,k) with $k = 0.03$, 0.01, and 0.05, and for the arrival time T, which corresponds to $p = p_c = 1/2$ according to Eq. (13). These arrival times are, respectively, $T = 4.95 \times 10^{-6}$, $T = 1.21 \times 10^{-16}$, and $T = 1.46 \times 10^{-32}$. The broken line indicates the scaling given in Eq. (15).

near criticality ($p \to p_c$) and for large clusters ($s \to \infty$):

$$n_s(p) = s^{-\tau} g[(p - p_c)s^{\sigma}], \tag{14}$$

where $g(z)$ is a scaling function that approaches a constant value for $|z| \ll 1$ and decays exponentially for $|z| \gg 1$. This scaling relation introduces a crossover size s_ξ, which scales as $s_\xi \sim |p - p_c|^{-1/\sigma}$, such that

$$n_s(p) \sim s^{-\tau} \quad \text{for} \quad s \ll s_\xi. \tag{15}$$

Beyond s_ξ, the power-law behavior fails, and the number of clusters decays fast. In two dimensions we have $\tau = 187/91$ and $\sigma = 36/91$.

In an FPP framework we do not have access to this number of clusters. Yet, given a fixed arrival time T, we can estimate the probability that the FPP ball contains exactly s sites, denoted here by $W_s(T)$. Since the center node always belongs to the FPP ball, this value can be mapped, in the percolation language, to the probability that a randomly chosen *cluster* site will be part of a cluster of size s. Let $w_s(p)$ be the probability (in the percolation problem) that the cluster to which a randomly chosen occupied site belongs has size s. It is easy to show that $n_s(p) = p\, w_s(p)/s$. We can now relate $W_s(T)$ and $w_s(p)$ through the mapping between arrival times and occupation probabilities given in Eq. (12), so we have $w_s(p(T)) = W_s(T)$. Thus, for a given arrival time T, we propose that our FPP ball distribution is given by

$$n_s(p(T)) = \frac{p(T)\, W_s(T)}{s}. \tag{16}$$

Our analysis of the statistics of the FPP balls begins in Fig. 5, in which we show the ball size distribution calculated from Eq. (16) for the three Weibull distributions of reference and for arrival times corresponding to the critical probability $p_c = 1/2$. We first observe a perfect collapse of the three curves into the scaling law given in Eq. (15) along several orders of magnitude. In bond percolation, the cutoff size s_ξ diverges at p_c, so we should expect a continuous power-law decay. However, the plot shows that distributions deviate from the naively predicted scaling after a given point, showing first an increase with respect to the expected values and then they decay very fast. Let us denote this cutoff size by $s_k(p)$, where we have assumed that, beyond its dependence on the order factor k, it also depends on the probability p. It it clear that this crossover size increases as the disorder becomes stronger, which leads us to conjecture that it diverges as $k \to 0$ for any p.

The crossover size s_k appears as a consequence of the breakdown of our main assumption: the max principle given in Eq. (11). Let us associate a length scale to s_k, given, for example, by the average radius of the balls of size s_k, and denote it by ξ_k. For length scales of the order of ξ_k the geodesic paths are long enough to include links with crossing times that, while smaller than the largest term, do significantly contribute to the arrival time. This means that, for a given arrival time T, not all the links with a crossing time lower than T are allowed, which leads to the breakdown of the max principle. As a result, the clusters with sizes larger than s_k predicted by percolation theory are trimmed into FPP balls with smaller sizes, a fact that leads to the increase of n_s for $s > s_k$ displayed in the figure. We will refer to this process as the *round-off* effect. For larger length scales and thus longer geodesics ($s \gg s_k$), the round-off effect limits the size of the distributed balls at a given arrival time T and the distribution drops steeply.

To see clearly this effect we can consider the critical point in bond percolation, where an infinite percolation cluster appears. Let us define the arrival time corresponding to the percolation threshold as the *critical arrival time* T_c: $T_c \equiv T(p_c)$. For the Weibull distribution we obtain $T_c = \lambda(\ln 2)^{1/k}$. An infinite ball $B(T_c)$ would necessarily imply infinitely long geodesics with an infinite number of links. Since link times are positive we cannot observe an infinite ball for a finite arrival time. Only for distributions with $F(0) = p_c$ (critical FPP) or $F(0) > p_c$ (supercritical FPP) we can observe infinite balls.

We can thus identify ξ_k as the length scale characterizing the crossover observed in the model: for length scales much smaller than ξ_k the behavior is the same as in bond percolation with $p = F(T)$.

At length scales of the order of ξ_k, we may postulate the existence of an equivalent bond-percolation problem characterized by an effective probability smaller than $p = F(T)$, because not all links with times below T are allowed. The upper limit of the integral given in Eq. (12) can no longer be given by T, but by $T - \epsilon_T$ with some $\epsilon_T > 0$. We conjecture that this results in an *effective* critical probability $p_{c,\text{eff}}$ which is slightly larger than the theoretical percolation threshold $p_c = 1/2$. A rough argument for this is as follows. Let us consider the inverse problem and fix the occupation probability p in the bond-percolation problem. Following the above reasoning we should expect that the effective arrival time T_{eff} of the equivalent FPP problem should be of the form $T_{\text{eff}}(p) = T(p) + \epsilon_T(p)$, with $T(p) = F^{-1}(p)$ and some $\epsilon_T(p) > 0$. At the critical point p_c we can then write $T_{c,\text{eff}}(p_c) = T(p_c) + \epsilon_T(p_c) = T_c + \epsilon_T(p_c)$. We can now define the *effective* critical probability $p_{c,\text{eff}}$ as the probability that satisfies

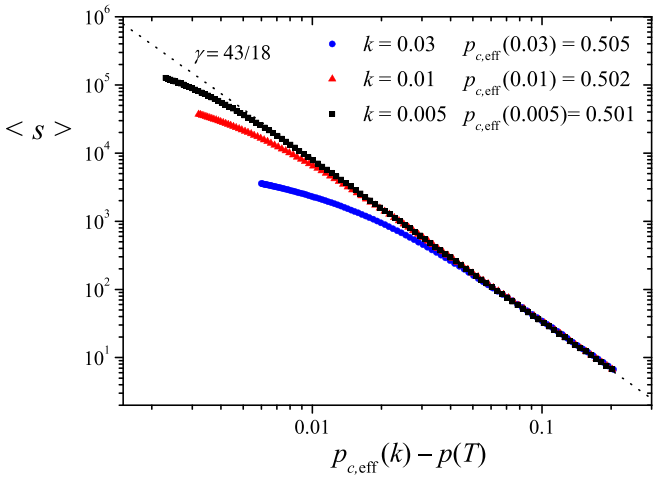

FIG. 6. Average cluster size of the FPP balls calculated from Eq. (18) as a function of $p_{c,\mathrm{eff}}(k) - p(T)$ for the three reference distributions. Corresponding $p_{c,\mathrm{eff}}(k)$ are shown in the legend. The straight broken line corresponds to the theoretical scaling given in Eq. (17).

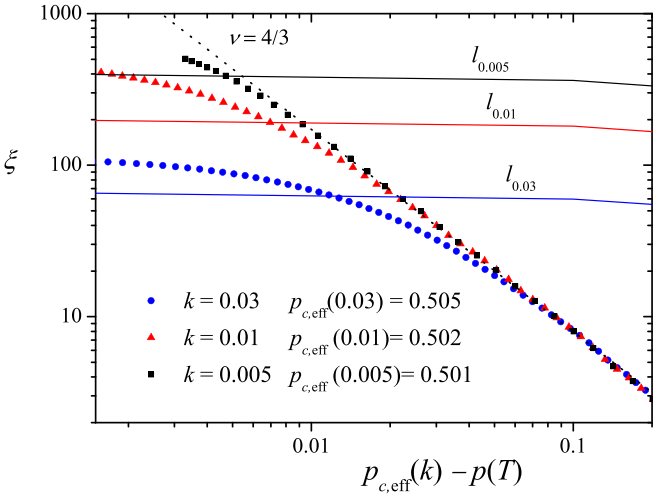

FIG. 7. Correlation length of the FPP balls calculated from Eq. (23) as a function of $p_{c,\mathrm{eff}}(k) - p(T)$ for the three reference distributions. Corresponding $p_{c,\mathrm{eff}}(k)$ values are shown in the key. Straight broken line corresponds to the theoretical scaling given in Eq. (21). Continuous curves correspond to the length $\ell_k(T(p))$ obtained for each k from the chain model presented in Sec. V.

$T(p_{c,\mathrm{eff}}) = T_{c,\mathrm{eff}}(p_c)$. We then have $p_{c,\mathrm{eff}} = F(T_{c,\mathrm{eff}}(p_c)) = \int_0^{T_{c,\mathrm{eff}}(p_c)} f(t)\,dt = \int_0^{T_c+\epsilon_T(p_c)} f(t)\,dt = p_c + \epsilon_p$, where $\epsilon_p = \int_{T_c}^{T_c+\epsilon_T(p_c)} f(t)\,dt > 0$.

It is expected that $p_{c,\mathrm{eff}}$ will depend on the order factor. To obtain the effective critical probability for each k we have represented the ball size distribution $n_s(p)$ obtained at different values of $p(T)$, and we have identified the value of p at which the cutoff value $s_k(p)$ where the ball distribution departs from the theoretical scaling law takes its maximum value (i.e., $p_{c,\mathrm{eff}}$ yields the largest value of s for which n_s still lies on the straight line). For case $k = 0.03$ we have observed that the maximum cutoff value is obtained at $p \approx 0.505$, so we have $p_{c,\mathrm{eff}}(0.03) \approx 0.505$. Repeating the procedure for cases $k = 0.01$ and $k = 0.005$ we obtain $p_{c,\mathrm{eff}}(0.01) \approx 0.502$ and $p_{c,\mathrm{eff}}(0.005) \approx 0.501$. Although the process is not rigorous and these values are far from being accurate, their validity can be checked in the collapses shown in the following discussion (Figs. 6, 7, and 8). It is very common in percolation studies to consider an effective critical probability different from the theoretical value in order to take into account finite-size effects. In our model these finite size effects appear as a consequence of the fact that the max principle given in Eq. (11) does not hold strictly. We expect that $p_{c,\mathrm{eff}}(k) \to p_c$ as $k \to 0$.

B. Average cluster size

In percolation theory the average cluster size $\langle s(p)\rangle$ is usually defined [31] as the first moment of the size distribution obtained from the random selection of some cluster site [defined above as $w_s(p)$]. We then have $\langle s(p)\rangle = \sum_s s\, w_s(p)$. As we approach criticality from below ($p \to p_c^-$) the average cluster size diverges according to the following scaling law:

$$\langle s(p)\rangle \sim |p_c - p|^{-\gamma}, \tag{17}$$

with the critical exponent $\gamma = 43/18$ for $D = 2$. This relation also holds when we approach the critical point from above ($p \to p_c^+$) provided that we exclude the single infinite cluster in the sum over all cluster sizes.

We can then calculate the average FPP-ball size in a similar way:

$$\langle s(p(T))\rangle = \sum_s s\, W_s(T). \tag{18}$$

Numerical evidence that the balls of the FPP model also obey the above scaling is shown in Fig. 6, where we have used the effective critical probabilities discussed above. For values of p much smaller than the critical value we observe an excellent collapse of the three curves into the expected power law. When p is close to the critical point the main contribution to the sum comes from large values of s. In percolation theory the size of these clusters is s_ξ, which diverges at the critical point. In our model we have found another crossover size, s_k, above which the round-off prevents balls with larger sizes. The interplay between both characteristic sizes can explain the behavior obtained in our simulations. For probabilities such that $s_\xi(p) \ll s_k(p)$ the round-off does not affect the dominating size $s_\xi(p)$ and FPP balls scale as percolation clusters. As p approaches the critical point, s_ξ diverges becoming larger than s_k, which now turns into the size that dominates the moments of the mass distribution. This yields smaller average sizes and thus a deviation with respect to the theoretical scaling. The crossover probability $p_k^\star$ (crossover arrival time $T_k^\star$) at which it occurs is thus obtained when $s_\xi(p_k^\star)$ is of the same order as $s_k(p_k^\star)$. In the previous section we obtained that s_k increases as the disorder becomes stronger, so $p_k^\star$ should also increase as k decreases, in agreement with the behavior displayed in the figure. We can thus expect that $p_k^\star \to p_c$ as $k \to 0$.

C. Correlation length

Critical behavior in percolation theory is completely dominated by a single characteristic length, the *correlation length* ξ

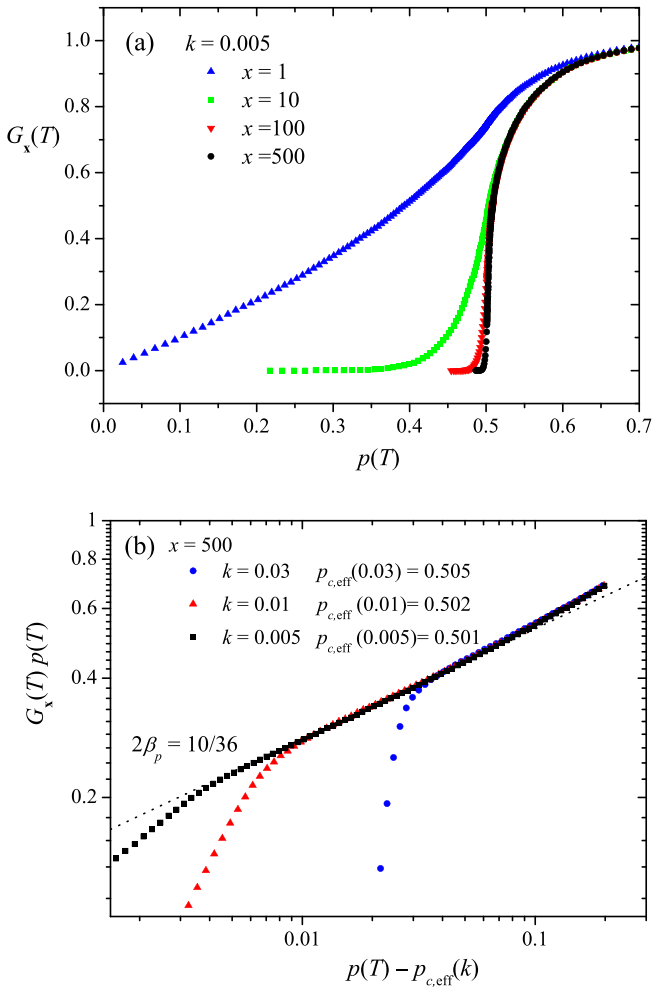

FIG. 8. Strength of the infinite cluster. (a) Probability that a node at position x in the axis will belong to the ball with passage time T, as a function of $p = F(T)$ for $k = 0.005$ and different distances: $x = 1$, 10, 100, and 500. (b) $G_{\mathbf{x}}(T)\,p(T)$ product as a function of $p(T) - p_{c,\mathrm{eff}}(k)$ for a node at $x = 500$ and the three reference distributions. The straight broken line represents the scaling behavior deduced in Eq. (26).

[31], which stands for the crossover length scale below which the behavior is indistinguishable from that at p_c.

Given a single percolation cluster, its *radius of gyration* is defined by the average squared distance between two cluster sites:

$$R_s^2 \equiv \frac{1}{2}\sum_{i,j}\frac{|\mathbf{r}_i - \mathbf{r}_j|^2}{s^2}, \tag{19}$$

where $\mathbf{r}_i$ stands for the position vector of the ith site of the cluster and the subscript s stands for the cluster size. We can average this radius over all clusters of size s to obtain $\overline{R_s^2}$. Finally, the average of $\overline{R_s^2}$ over all cluster sizes s in the following way provides a standard definition of the squared correlation length [31]:

$$\xi^2(p) \equiv 2\frac{\sum_s \overline{R_s^2} s^2 n_s(p)}{\sum_s s^2 n_s(p)}, \tag{20}$$

which is known to diverge as we approach the critical point ($p \to p_c$) as

$$\xi(p) \sim |p_c - p|^{-\nu}, \tag{21}$$

with $\nu = 4/3$ for $D = 2$. Again, if we approach from above we have to exclude in the sum the contribution of the infinite cluster.

The correlation length is the radius of those clusters which mainly contribute to the second moment of the cluster size distribution. Near the percolation threshold this contribution comes from the clusters of size of the order of s_ξ, so we find

$$s_\xi \sim \xi^{D_f}, \tag{22}$$

where D_f is the fractal dimension of the infinite percolation cluster, $D_f = 91/48$ for $D = 2$.

If we turn now to our FPP problem and apply the equivalence discussed so far to Eq. (20), we deduce the following expression for the correlation length of the FPP balls:

$$\xi^2[p(T)] = 2\frac{\sum_s \overline{R_s^2}\, sW_s(T)}{\sum_s sW_s(T)}. \tag{23}$$

Results regarding the correlation length are displayed in Fig. 7 following the same scheme as in Fig. 6 for the average size. The similarity between both plots is not surprising since they correspond to moments of the same cluster size distribution. According to percolation theory, s_ξ is exactly the cluster size that dominates the moments of the mass distribution, including the average cluster size $\langle s\rangle$ and the correlation length ξ. As a consequence, ξ represents the radius of the clusters of size s_ξ. On the other hand, the radius ξ_k of balls of size s_k gives the crossover length scale below which the balls behave as percolation clusters. We can thus use here the explanation given for the average cluster size by considering the correlation length ξ instead of s_ξ, and the cutoff radius ξ_k instead of s_k. For probabilities such that $\xi(p) \ll \xi_k(p)$, the round-off effect is negligible since it affects only sizes much larger than the dominant size s_ξ. Thus, the correlation length of the FPP balls behaves as in the percolation problem. As we approach the critical point, ξ diverges, becoming much larger than ξ_k. Due to the round-off effect, size s_k becomes the dominant term, yielding a deviation with respect to the scaling law. The crossover probability $p_k^\star$ is the same as for the average cluster size and is obtained when $\xi(p_k^\star)$ is of the same order as $\xi_k(p_k^\star)$.

D. Percolation probability

The order parameter of the second-order phase transition observed in percolation is given by the *percolation probability* $\mathcal{P}$, or *strength of the infinite cluster*, defined as the probability that a randomly chosen site belongs to the infinite cluster. For $p \leqslant p_c$ we have $\mathcal{P} = 0$, and it goes to zero as a power law as we approach the critical point from above ($p \to p_c^+$):

$$\mathcal{P}(p) \sim (p - p_c)^{\beta_p}, \tag{24}$$

where $\beta_p = 5/36$ for $D = 2$ is yet another critical exponent [31]. Our purpose is to recover this exponent from the analysis of the FPP balls.

Let us define $G_{\mathbf{x}}(T)$ as the probability that site $\mathbf{x}$ belongs to the FPP ball at passage time T,

$$G_{\mathbf{x}}(T) = \text{Prob}\{\mathbf{x} \in B(T)\}. \tag{25}$$

$G_{\mathbf{x}}(T)$ is also the probability that the arrival time needed to reach site $\mathbf{x}$ is less than T, i.e., the cumulative distribution of the arrival time to node $\mathbf{x}$ at time T. Note that $G_{\mathbf{x}}(T)$ is related to the probability density function $g_{\mathbf{x}}(T)$ addressed in previous section and displayed in Fig. 3, through $g_{\mathbf{x}}(T) = dG_{\mathbf{x}}(T)/dT$. The behavior of $G_{\mathbf{x}}(T)$ as a function of $p = F(T)$ for different sites along the axis for $k = 0.005$ is shown in Fig. 8(a).

As we move away from the center node the curves become sharper around $p = 1/2$ and, for large x, $G_{\mathbf{x}}(T)$ tends to a limit function. That limit function is qualitatively very similar to the plot of the order parameter $\mathcal{P}$ as a function of p. For distant positions there is a minimum arrival time, which approaches very fast the critical passage time T_c as $x \to \infty$. This result is consistent with the criticality of the percolation problem: at $p = p_c$ an infinite cluster that percolates through the lattice appears for the first time.

From these results and Eq. (25) we deduce that for $x \gg 1$, $G_{\mathbf{x}}(T)$ is the probability that both the initial and the final points belong to the infinite cluster. In percolation theory this probability is given, for very long distances (and thus uncorrelated sites), by $\mathcal{P}^2$. Besides, this probability is conditioned on the known fact that the initial point (the center node) belongs to the cluster, so we have to divide the above expression by p. Our reasoning allows us to conjecture that for $x \gg 1$,

$$G_{\mathbf{x}}(T) \approx \frac{\mathcal{P}^2(p)}{p} \to \frac{(p - p_c)^{2\beta_p}}{p} \quad \text{as} \quad p \to p_c, \tag{26}$$

using always $p = F(T)$. Numerical evidence for Eq. (26) is shown in Fig. 8(b). The plot displays the values of the product $p\,G_{\mathbf{x}}(T)$, obtained from Fig. 8(a), as a function of $p - p_{c,\text{eff}}(k)$, for the three levels of disorder. As in previous figures we obtain an excellent collapse of the curves into the expected power law as $p \to p_{c,\text{eff}}(k)$, while deviations take place at the same crossover probabilities $p_k^\star$ obtained before for the mean cluster size and the correlation length.

E. Fractal dimension of FPP balls

The infinite cluster at the critical point is a fractal, so its mass M scales with the linear size ℓ as $M \sim \ell^{D_f}$, where D_f is the *fractal dimension* ($D_f = 91/48$ for two dimensions). However, fractal behavior is also observed away from the critical point at length scales much smaller than the correlation length, so we have $M \sim \ell^{D_f}$ for $\ell \ll \xi$, and $M \sim \ell^{D'}$ for $\ell \gg \xi$, with dimension D' depending on whether we are above or below the critical point (for $p > p_c$ we have $D' = D$, the Euclidean dimension). Clusters look fractal on scales smaller than ξ, and this also applies to the relation between their mass s and their linear size R_s: for $R_s \ll \xi$ or equivalently $s \ll s_\xi$ we find $s \sim R_s^{D_f}$, from which we can deduce Eq. (22).

In Fig. 9 we have shown the mass of FPP balls within circles of increasing radius r centered at the origin, for extreme disorder $k = 0.005$. To perform the analysis we have selected among all the FPP balls grown at critical passage time T_c those with sizes contained in small intervals around three different sizes s. Results were averaged over all the balls within the same interval.

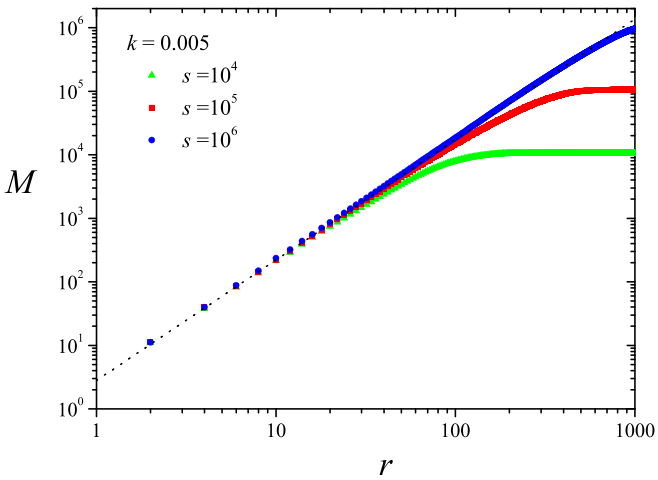

FIG. 9. Mass of the FPP ball $B(T_c)$ within a circle of radius r centered at the origin for case $k = 0.005$. Results are the average over balls with sizes within the following intervals: (green) $s \in (1, 1.1) \times 10^4$, (red) $s \in (1, 1.1) \times 10^5$, and (blue) $s \in (1, 1.1) \times 10^6$. The straight line corresponds to the power law $M \sim r^{91/48}$.

The plots show a constant slope which coincides with the fractal dimension for critical percolation (broken line). The final plateaus are due to the fact that clusters are finite with linear size R_s, so after $r \approx R_s$ the mass becomes constant. It is interesting to note that sizes $s = 10^5$ and $s = 10^6$ are larger than the corresponding cutoff size s_k (above 10^4; see Fig. 5), i.e., these clusters are influenced by the round-off. However, this effect does not seem to significantly change the internal structure of the balls, which is still fractal, so the main consequence of the round-off is the trimming of the branched edges.

V. CROSSOVER LENGTH FOR PERCOLATION IN THE FPP MODEL

Let us elaborate on the validity of the max principle that allows the mapping of the FPP into the percolation problem. Our purpose is to find an estimate for the cutoff values $\xi_k(p)$ and $s_k(p)$. The same discussion can be extended to the other distributions in Sec. II, making use of the suitable order factor ω (k, σ^{-1} or α respectively for Weibull, log-normal, or Pareto).

A different way to characterize the max principle is presented in the following experiment, which we call the *chain model*. Let us consider a linear array of ℓ sites and let us choose a time T. Then we fill the chain with the values of t obtained by sampling the link-time distribution, but keeping only those values which are smaller than T, i.e., if $t \geqslant T$ we disregard the value. These chains represent idealized versions of the minimal paths since they cannot include crossing times larger than the passage time T. We define $\mathbf{P}$ as the probability for the sum of the link times to be smaller than T:

$$\mathbf{P}_k(\ell, T) = \text{Prob}\left\{\sum_{i=1}^{\ell} t_i < T \mid t_i < T\right\}. \tag{27}$$

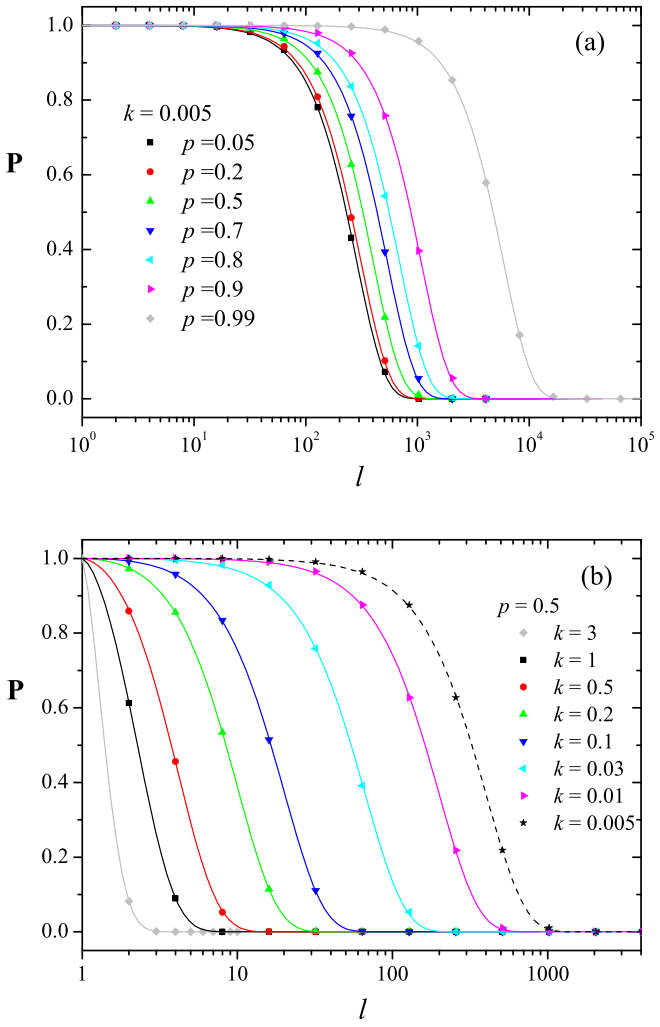

FIG. 10. Probability **P** calculated from Eq. (27) over an ensemble of 10^6 chains as a function of the chain length ℓ for (a) $k = 0.005$ and different passage times represented by $p(T)$ and (b) $p = 0.5$ and different k. Points correspond to results from simulations, and continuous lines represent the corresponding fits to function in Eq. (29).

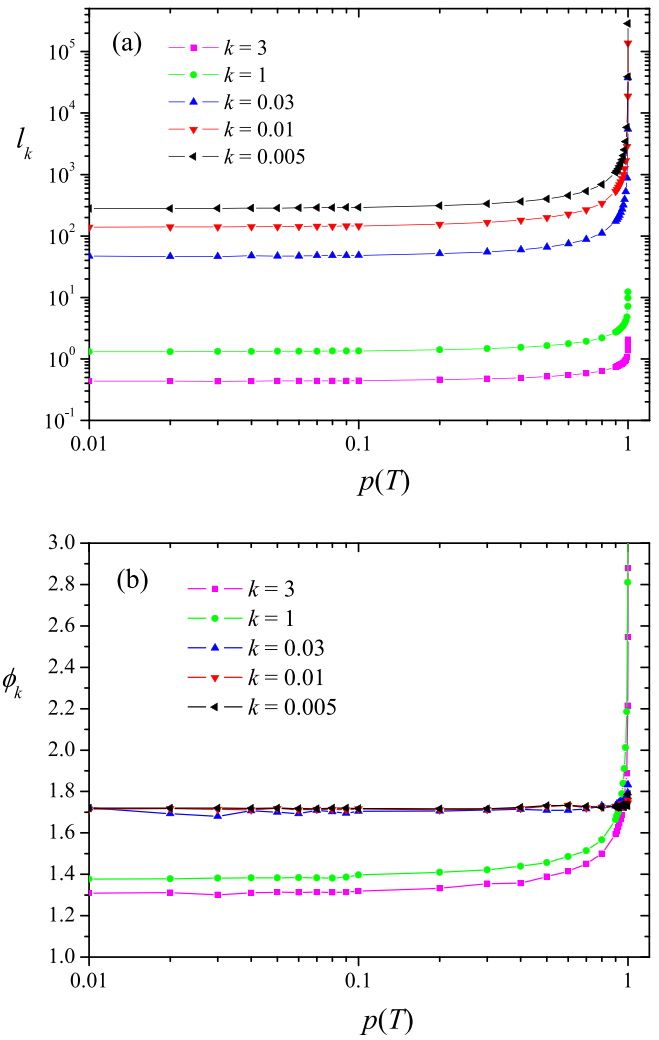

FIG. 11. Fitted values of the cutoff length $\ell_k(T)$ (a) and the stretch exponent $\phi_k(T)$ (b) as a function of probability $p(T)$ for different order factors.

$\mathbf{P}_k(\ell, T)$ can be seen as the probability that the max principle holds at a length scale ℓ and passage time T. Our claim is the following: if there exists a cutoff length $\ell_k(T)$ such that

$$\mathbf{P}_k(\ell, T) \approx \begin{cases} 1 & \text{for } \ell \ll \ell_k(T), \\ \text{fast decay} & \text{for } \ell \gg \ell_k(T), \end{cases} \tag{28}$$

then $\xi_k(p)$ should behave as $\ell_k(T)$, always with $p = F(T)$. It is important to stress that the dependency on k of $\ell_k(T)$ and $\mathbf{P}_k(\ell, T)$ is actually a functional dependency. The numerical evidence that follows will support our claim.

Figure 10 shows two sets of results for $\mathbf{P}_k(\ell, T)$. In Fig. 10(a) we display the dependence of **P** on ℓ for different arrival times T [expressed as $p(T)$] and for fixed $k = 0.005$. In Fig. 10(b) the arrival time has been fixed to T_c, and the curves correspond to different strengths of the disorder (different values of k).

The first remarkable result is that $\mathbf{P}_k(\ell, T)$ shows an excellent agreement with the *stretched exponential function*:

$$\mathbf{P}_k(\ell, T) \approx \exp\left\{-\left[\frac{\ell - 1}{\ell_k(T)}\right]^{\phi_k(T)}\right\}. \tag{29}$$

The corresponding fits have been indicated with colored continuous lines. As shown, the dependence of **P** on ℓ follows the behavior conjectured in Eq. (28) with $\ell_k(T)$ thus playing the role of a cutoff length. It is important to stress that we have obtained the same behavior for the other link-time distributions investigated in this work (log-normal and Pareto).

We address now the behavior of the fitting parameters, the cutoff length $\ell_k(T)$ and the stretch exponent $\phi_k(T)$, displayed in Figs. 11(a) and 11(b), respectively, as a function of the probability $p(T)$ for different values of the order factor k.

With regard to $\ell_k(T)$, our results support all the assumptions made in the previous section about ξ_k. For a given arrival time it increases monotonously with the disorder, and for a given disorder it is a continuously increasing function of the arrival time. We expect $\ell_k(T)$ to diverge for any arrival time as

$k \to 0$. Interestingly, although $\ell_k(T)$ is not defined at $T = 0$ it shows a well-defined positive limit. The same was found for the log-normal distribution while for Pareto the limit is 0.

Another remarkable result is the change of behavior near the crossover point between weak and strong disorder ($k^\star = 1.79$). For $k < k^\star$ we obtain $\ell_k(T) > 1$ for all T, consistent with our assumption that under strong disorder conditions there is always a length scale below which the FPP model behaves as a percolation lattice. However, if $k > k^\star$ (see, e.g., case $k = 3$) the fitted values of $\ell_k(T)$ are smaller than 1 for $p < 1$. Indeed, as k increases above $k^\star$ the decay of $\mathbf{P}_k(\ell, T)$ after $\ell = 1$ becomes sharper and the expression given in Eq. (28) approaches the step function: $\mathbf{P}_k(\ell, T) = 1$ if $\ell = 1$ and $\mathbf{P}_k(\ell, T) = 0$ if $\ell > 1$. As a consequence, the fitted values of $\ell_k(T)$ approach 0 as k increases for finite T (or $p < 1$). We can then expect that actual function $\ell_k(p) - 1$ approaches the δ function $\delta(1 - p)$ as $k \to \infty$. We will return to this issue later when we address the homogeneous case. Nevertheless, the change of behavior of $\ell_k(T)$ near the crossover point $k^\star$ points to it as a reliable estimate for the crossover length ξ_k.

With regard to the stretch exponent $\phi_k(T)$, displayed in Fig. 11(b), we observe that for a given p it increases with disorder and seems to approach a constant value above 1.7 under strong disorder conditions. We also notice that, in this regime, it roughly remains constant with p. Only for large k do we observe a smooth increase with passage time that sharpens as we approach $p = 1$.

In order to check the relation between the cutoff length ℓ_k obtained from our chain model and the crossover length ξ_k, which was postulated as the length scale under which the FPP model behaves as bond percolation, we have represented the corresponding curves of ℓ_k in the plot of the correlation length ξ of the FPP balls in Fig. 7. The comparison between both magnitudes provides numerical evidence of our claims. For probabilities p such as $\xi \ll \ell_k$, the correlation length of the balls follows the scaling behavior predicted from percolation theory. As p increases and ξ approaches ℓ_k, the effect of the round-off makes ξ depart from the percolation prediction. As discussed, this deviation takes place at $p_k^\star$, where both quantities become of the same order. A crossover towards an alternative behavior that its controlled by ℓ_k takes place, in which we expect that ξ will grow as ℓ_k for $p \gg p_k^\star$.

We can provide further numerical evidence of the reliability of ℓ_k as an estimator for the crossover length ξ_k. For example, we can conjecture that ℓ_k is the radius of the balls with cutoff-size s_k, so we can expect

$$s_k \sim \ell_k^D. \tag{30}$$

Then, according to Eq. (15), the number of clusters of size s_k, n_{s_k}, must behave as

$$n_{s_k} \sim s_k^{-\tau} \sim \ell_k^{-\tau D}. \tag{31}$$

For probabilities close to the percolation threshold so that $s_k \ll s_\xi$, the size distributions obtained from different k should collapse into a single universal curve if we rescale the size s by s_k, and n_s by n_{s_k}. That rescaling applied to the distributions displayed in Fig. 5 is shown in Fig. 12, and a quite satisfactory collapse of the three distributions is obtained.

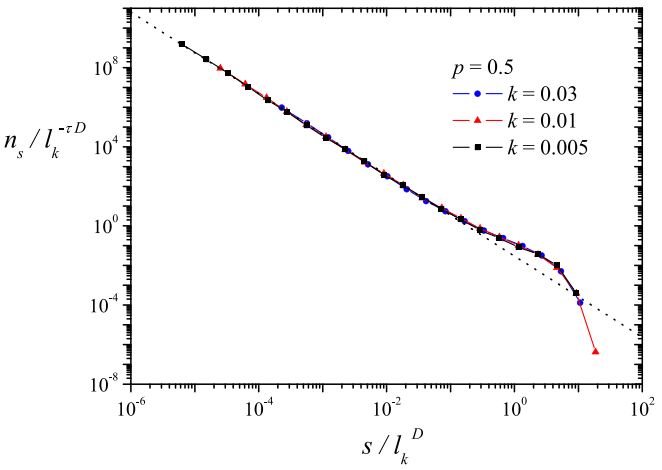

FIG. 12. Rescaling of the size distributions displayed in Fig. 5. For each curve, ball size s has been rescaled by ℓ_k^D ($D = 2$) with values $\ell_{0.03}(p = 0.5) = 65.83$, $\ell_{0.01}(p = 0.5) = 199.34$, and $\ell_{0.005}(p = 0.5) = 399.72$, obtained from the simulations of the chain model. n_s has been rescaled by $\ell_k^{-\tau D}$ according to Eq. (31).

VI. DISCUSSION: CROSSOVER BETWEEN PERCOLATION AND KPZ SCALING

For the sake of generality, we will use the generic order factor ω in the following discussion, which stands for the suitable parameter from the aforementioned distributions, i.e., k (Weibull), σ^{-1} (log-normal), or α (Pareto).

A. Strong disorder regime $\omega \ll \omega^\star$

The growth of FPP balls is controlled by two characteristic lengths: the crossover length ξ_ω which determines the length scale below which the FPP model is essentially a bond-percolation lattice with $p = F(T)$, and the correlation length ξ intrinsic to the percolation problem. Whereas the behavior of ξ is well known from percolation theory—at least close to the critical point—we can assume that the crossover length ξ_ω is related to the cutoff length ℓ_ω of the chain model. This is a strong assumption because the link times traversed by actual geodesics are correlated to each other by means of the minimal time principle, in contrast to the uncorrelated link times assumed in our model.

For distributions such as Weibull or log-normal, $\ell_\omega(T)$ has a well-defined positive limit when $T \to 0$, so we can expect the same for ξ_ω. Since ξ is initially 0, we conclude that FPP balls will display initial percolation-like growth provided this limit value is larger than 1. This seems to be guaranteed in the strong disorder regime $\omega \ll \omega^\star$. For the Pareto distribution we find $\ell_\omega(T) \to 0$ as $T \to 0$. However, the increase of $\ell_\omega(T)$ with passage time T is faster than the increase of $\xi(p)$ with probability $p(T)$, hence allowing the initial percolation phase.

Percolation-like growth will take place whenever ξ is much smaller than ξ_ω. We recall that both quantities increase monotonically with passage time. In this regime, the growth of the FPP balls with T can be mapped into the growth of the percolation clusters at increasing occupation probability $p = F(T)$. That regime continues until ξ becomes of the same order as ξ_ω, which takes place at a certain arrival time

$T_\omega^\star$. Since ξ diverges at the critical point $p_c = F(T_c)$, this crossover time is upper bounded by the critical passage time: $T_\omega^\star < T_c$. Under extreme disorder conditions, i.e., for small but positive values of the order factor ω, ξ_ω is large, $T_\omega^\star$ is close to T_c, and we can observe the fractal clusters obtained in percolation. We expect that $T_\omega^\star \to T_c$ as $\omega \to 0$, i.e., for infinite disorder.

Once the crossover arrival time $T_\omega^\star$ has been reached, we enter into a transient regime that evolves towards KPZ scaling. Above $T_\omega^\star$ two different types of growth at two different length scales take place simultaneously. At scales below ξ_ω, percolation-like growth still continues. The increase of p above p_c fills the inner holes and cavities and smooths the irregularities of the outer perimeter. However, the cutoff length ξ_ω prevents the incipient infinite percolation cluster from spreading along the lattice. At larger scales the growth of the ball is controlled by the growth of ξ_ω, which simply reflects the fact that minimal paths are limited by their length. FPP balls becomes compact with a regular shape, a process that finally leads to KPZ scaling.

This transient regime would last until the effects of percolation vanish, i.e., when $p = 1$, which corresponds to an infinite arrival time. We can speculate, however. For example, in Fig. 4 we showed the fluctuations of the arrival time to points along the axis for different levels of disorder. At this point we already know that $k = 0.5$, 0.3, or 0.2 are not small enough to display the criticality of percolation, but the disorder is in fact strong enough to reveal percolation effects in the behavior of the arrival-time fluctuations. In each curve of the figure with $k < k^\star$ we have marked three representative lengths obtained from the chain model. As an approximation of ξ_k we have considered $\ell_k(T_c)$, indicated with the vertical segments. In order to estimate the range of the percolation effects, and hence the crossover towards KPZ scaling, we have represented in each curve with a gray rectangle the interval $[\ell_k(T(p = 0.99)), \ell_k(T(p = 0.999))]$. Despite the approximations and the simplicity of our model, the crossover points are in a reasonably good agreement with the behavior displayed by the fluctuations.

Both the crossover length ξ_ω and the associated cutoff size s_ω increase with disorder, and we expect them to diverge as $\omega \to 0$. The kinetics of the approach towards *infinite* disorder depends on the specific distribution. For example, for the Weibull distribution we obtain the following limit of Eq. (13), valid for $p \in [0, 1)$:

$$\lim_{k\to 0} T(p) = \begin{cases} 0 & \text{if } p < p_0 \\ \lambda & \text{if } p = p_0 \\ \infty & \text{if } p > p_0 \end{cases}, \tag{32}$$

where $p_0 = 1 - e^{-1} = 0.63$. After an infinitesimal arrival time the balls take the form of the percolation clusters obtained at $p = p_0$. This is followed by an infinitely slow growth. At the limit we have $B(T) = B(0)$ for $T > 0$, where $B(0)$ is the percolation cluster obtained at $p = p_0$.

For the log-normal distribution we have

$$T(p) = e^\mu \exp\left(\sqrt{2\sigma^2}\,\mathrm{erf}^{-1}[2p - 1]\right), \tag{33}$$

where $\mathrm{erf}^{-1}(x)$ is the inverse error function, and the approach to the critical point is similar:

$$\lim_{\sigma\to\infty} T(p) = \begin{cases} 0 & \text{if } p < p_0 \\ e^\mu & \text{if } p = p_0 \\ \infty & \text{if } p > p_0 \end{cases}, \tag{34}$$

but now we have $p_0 = 1/2$, i.e., the critical ball is just the critical percolation cluster obtained at the critical probability.

Finally, for the Pareto distribution we have

$$T(p) = t_m \left(\frac{1}{1-p}\right)^{1/\alpha}, \tag{35}$$

and we obtain

$$\lim_{\alpha\to 0} T(p) = \infty \quad \text{for } 0 < p < 1, \tag{36}$$

which means that we must resort to increasingly large arrival times in order to observe the growth.

B. Weak disorder regime $\omega \gg \omega^\star$

It is interesting to finish this work by considering the opposite limit $\omega \to \infty$ of *infinite* order, which is given by the homogeneous case in which all links have the same crossing time τ_0. As discussed in Sec. II, this case corresponds to the limit $\omega \to \infty$ of the link-time distributions, even though the specific value of τ_0 depends on the distribution function [see Eq. (6)]: $\tau_0 = \lambda, e^\mu, t_m$ for Weibull, log-normal, and Pareto, respectively.

For the homogeneous case the chain model gives exactly $\ell_\omega(T) = T/\tau_0$. Now we can use the following result, which applies to all distributions:

$$\lim_{\omega\to\infty} T(p) = \tau_0 \quad \text{for } p < 1, \tag{37}$$

to obtain

$$\lim_{\omega\to\infty} \ell_\omega(p) = 1 \quad \text{for } p < 1. \tag{38}$$

It is important to note that this limit strictly holds for probabilities smaller than 1. At the limit $p \to 1$ we obtain $\ell_\omega \to \infty$.

This result confirms the assumption made in the previous section,

$$\lim_{\omega\to\infty} \ell_\omega(p) - 1 = \delta(1 - p), \tag{39}$$

and shows that for a weak enough disorder we cannot observe the percolation phase because it extends to only a few sites.

As a numerical example, let us consider the distribution Wei(1,3) where value $k = 3$ is above the crossover value $k^\star \approx 1.79$. From the chain model we obtain $\ell_3(p = 0.99999) \approx 1.86$, which roughly means that percolation effects up to a probability of $p = 0.99999$ are limited to a length scale of less than two lattice units. On the other hand, the arrival time corresponding to that probability is $T(p = 0.99999) \approx 2.26$. Now we can use the value of the mean time for that distribution, $\tau \approx 0.89$ (close to $\tau_0 = \lambda = 1$), to obtain $T/\tau \approx 2.53$, i.e., around two lattice units, which provides a reasonable estimate of $\ell_3(p = 0.99999)$. This result shows that we cannot observe percolation effects even at disorders close to the crossover value $\omega^\star$.

VII. CONCLUSIONS AND FURTHER WORK

In this work we have characterized the dynamics of first-passage percolation (FPP) square lattices under extreme disorder, as opposed to the weak-disorder regime, which is dominated by KPZ universality. Several link-time distributions were considered which allow for a continuous variation of the disorder strength through the so-called *order factor* ω. A crossover value $\omega^\star$ (for which $d_c = 1$) was proposed as the crossover point between the two regimes.

Our study has revealed that, given a certain level of disorder, there exists a characteristic length scale ξ_ω below which the FPP model behaves essentially as a bond-percolation lattice. Arrival times at length scales smaller that ξ_ω follow a max principle which allows us to establish a continuous mapping of FPP passage time T into the probability p of a bond being open in bond percolation. The basic assumption is that the sum of link times along the geodesic can be approximated by their maximum value. As a result the mapping has the form $p = F(T)$, where F denotes the cumulative distribution function for the link times.

At length scales below ξ_ω the FPP model displays the same criticality found in the second-order phase transition associated to bond percolation. The average value of the arrival time to different sites becomes ill-defined, and the geodesic between neighboring points of the lattice can become arbitrarily large, instead of using a single link as in the weak-disorder regime. Through a comprehensive scaling analysis of the FPP balls we have been able to observe the critical exponents characterizing the scaling of the percolation clusters near the critical point, including their fractal structure, instead of the reasonably rough circular balls within the KPZ universality class.

The dynamics of the FPP growth under strong disorder conditions is the result of the interplay between this crossover length ξ_ω and the correlation length ξ characteristic of bond percolation, both evolving dynamically with passage time T. When $\xi \ll \xi_\omega$ the growth of the FPP balls with passage time T can be mapped into the growth of the percolation clusters with increasing probability $p = F(t)$, which resembles a sort of *invasion percolation*. At a certain passage time $T^\star_\omega$ (which is upper bounded by the critical arrival time T_c), ξ becomes of the same order of ξ_ω. Further growth leads to the failure of the maximality assumption: the sum of the link times along a geodesic may become significantly different from the maximal value found along it. Thus balls must start a rounding-off process that yields a crossover towards KPZ scaling. Therefore, for long enough distances we always recover the KPZ regime.

The crossover length ξ_ω, as well as other related magnitudes defined as a function of the order factor ω, increases as the disorder becomes stronger and seems to diverge when the order factor approaches zero, which we call the *infinite-disorder* limit. The infinite-disorder limit of these models presents very intriguing features which might be related to *critical* or *supercritical* FPP cases and which we intend to ascertain in future work. We have provided very preliminary evidence pointing to that idea. Note, for example, that limit when $\omega \to 0$ of the Weibull and log-normal distribution functions given in Eqs. (3) and (4) are, for nonzero t, $F(t) = 1 - e^{-1} = 0.63$ and $F(t) = 1/2$, respectively. They have the form of the Bernoulli distribution (except for $t = 0$) in which link times can be zero (open bonds) with probability p_0 and infinite (closed bonds) with probability $1 - p_0$, with p_0 given by the above values. For the Weibull distribution we have $p_0 > p_c$, and its infinite-disorder limit might be related to supercritical FPP, whereas for the log-normal we have $p_0 = p_c$ and thus the critical case. Since length ξ_ω determines the crossover length scale between percolation and KPZ phases, and it diverges at the infinite-disorder limit, certainly it would be very interesting to study the criticality near this limit.

Another direction of future work is to elaborate more on the estimate for ξ_ω derived from the chain model. Although the numerical evidence presented here supports its validity, there are still many open questions that deserve additional

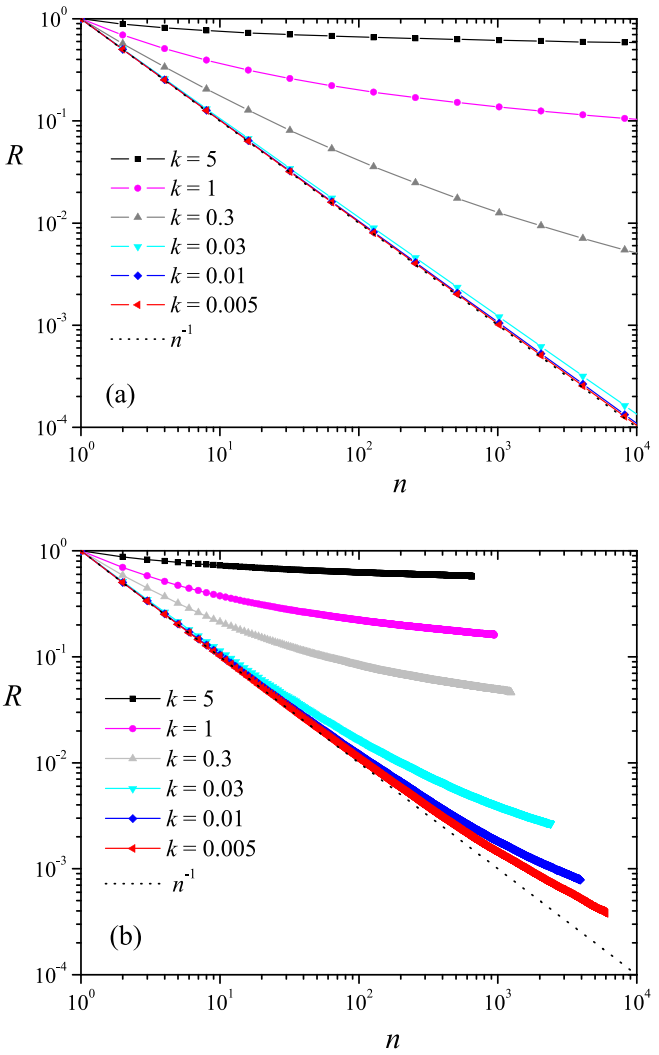

FIG. 13. Value of R calculated from Eq. (A2) and averaged over 10^4 realizations, as a function of length n for (a) a list of n independent values of t randomly sampled from the Weibull distribution with $\lambda = 1$ and different values of the order factor k and (b) actual geodesics of length n obtained in the FPP model with link times distributed in the same way. The theoretical behavior n^{-1} predicted from the exact fulfillment of the max principle has been indicated in both panels with the dotted line.

work, including a theoretical justification of Eq. (29) and the generalization of the observed behaviors to other link-time distributions.

ACKNOWLEDGMENTS

We thank R. Cuerno, E. Koroutcheva, and E. Rodríguez-Fernández for very useful discussions. Also, we acknowledge the Spanish government for financial support through grants FIS2015-66020-C2-1-P and PGC2018-094763-B-I00. D.V. acknowledges the Community of Madrid for the predoctoral contract PEJD-2018-PRE/IND-9095 co-funded by the European Social Fund (ESF) through the Youth Employment Operational Programme and the Youth Employment Initiative (YEI). I.A.D. acknowledges the Community of Madrid for the research contract PEJ-2018-AI/IND-10573 co-funded by the European Social Fund (ESF) through the Youth Employment Operational Programme and the Youth Employment Initiative (YEI).

APPENDIX: ON THE VALIDITY OF THE MAX PRINCIPLE

In Sec. IV we put forward a max principle that allowed us to propose a theoretical framework to characterize the percolation phase in the FPP model under strong disorder conditions. Equation (11) provides the statement for the aforementioned max principle. In order to check its validity we have considered the following ratio, defined for every link i traversed by a given geodesic:

$$R_i = \frac{t(\mathbf{x}_{i-1}, \mathbf{x}_i)}{\max_i\{t(\mathbf{x}_{i-1}, \mathbf{x}_i)\}}, \tag{A1}$$

with $i = 1, \ldots, n$ and where n is the length of the minimal path. The arrival time along that geodesic will be $T = \sum_{i=1}^{n} t(\mathbf{x}_{i-1}, \mathbf{x}_i)$, and if the max principle holds $T \approx \max_i\{t(\mathbf{x}_{i-1}, \mathbf{x}_i)\}$. Let us define now R as the average of R_i over all links belonging to that minimal path, so we have

$$R(n) = \frac{1}{n}\sum_{i=1}^{n} R_i = \frac{1}{n}\frac{T}{\max_i\{t(\mathbf{x}_{i-1}, \mathbf{x}_i)\}}. \tag{A2}$$

If the max principle holds, we then obtain

$$R(n) \approx n^{-1}, \tag{A3}$$

which allows us to statistically check the validity of the principle.

We first show that the applicability of the max principle is an intrinsic property of the link-time distribution. Figure 13(a) shows the value of R as a function of n, obtained from lists of n independent random times drawn from Weibull distributions with $\lambda = 1$ and different values of the order factor k. Each value has been averaged over an ensemble of 10^4 lists. It can be clearly seen that for low values of k, i.e., for strong levels of noise, the results follow the trivial relation given in Eq. (A3) (indicated in the figure with the dotted line). Actual geodesics, on the other hand, provide lists of random times which are correlated through the min principle stated in Eq. (2). Results for the geodesics obtained in the FPP model with the same link-time distributions have been displayed in Fig. 13(b). The qualitative behavior is the same, but if we focus on the strongest disorders (lowest values of the order factor k), we observe that the range of validity of the max principle decreases with respect to the case with independent times. The reason is that under strong disorder conditions, the min principle mainly affects to the term $\max_i\{t(\mathbf{x}_{i-1}, \mathbf{x}_i)\}$, as stated in Eq. (11), which is therefore minimized. This effect becomes more pronounced on longer geodesics, hence explaining the differences between both sets of results.

[1] D. Nelson, T. Piran, and S. Weinberg, *Statistical Mechanics of Membranes and Surfaces* (World Scientific, Singapore, 2004).
[2] D. H. Boal, *Mechanics of the Cell* (Cambridge University Press, Cambridge, 2012).
[3] C. Itzykson and J.-M. Drouffe, *Statistical Field Theory* (Cambridge University Press, Cambridge, 1991).
[4] B. Booß-Bavnbek, G. Esposito, and M. Lesch, *New Paths towards Quantum Gravity* (Springer, Berlin, 2009).
[5] J. Ambjørn, B. Durhuus, and T. Jonsson, *Quantum Geometry: A Statistical Field Theory Approach* (Cambridge University Press, Cambridge, 1997).
[6] S. N. Santalla, J. Rodriguez-Laguna, T. LaGatta, and R. Cuerno, Random geometry and the Kardar-Parisi-Zhang universality class, New J. Phys. **17**, 033018 (2015).
[7] S. N. Santalla, J. Rodriguez-Laguna, A. Celi, and R. Cuerno, Topology and the Kardar-Parisi-Zhang universality class, J. Stat. Mech. (2017) 023201.
[8] M. Kardar, G. Parisi and Y.-C. Zhang, Dynamic Scaling of Growing Interfaces, Phys. Rev. Lett. **56**, 889 (1986).
[9] A.-L. Barabási and H. E. Stanley, *Fractal Concepts in Surface Growth* (Cambridge University Press, Cambridge, 1995).
[10] J. Krug, Origins of scale invariance in growth processes, Adv. Phys. **46**, 139 (1997).
[11] T. Kriecherbauer and J. Krug, A pedestrian's view on interacting particle systems, KPZ universality and random matrices, J. Phys. A: Math. Theor. **43**, 403001 (2010).
[12] T. Halpin-Healy and K. Takeuchi, A KPZ Cocktail—Shaken, not stirred: Toasting 30 years of kinetically roughened surfaces, J. Stat. Phys. **160**, 794 (2015).
[13] M. Prähofer and H. Spohn, Scale invariance of the PNG droplet and the Airy process, J. Stat. Phys. **108**, 1071 (2002).
[14] K. A. Takeuchi, M. Sano, T. Sasamoto, and H. Spohn, Growing interfaces uncover universal fluctuations behind scale invariance, Sci. Rep. **1**, 34 (2011).
[15] I. Corwin, J. Quastel, and D. Ramenik, Continuum statistics of the Airy$_2$ process, Commun. Math. Phys. **317**, 347 (2013).
[16] J. M. Hammersley and D. J. A. Welsh, First-passage percolation, subadditive processes, stochastic networks and generalized renewal theory, in *Bernoulli, Bayes, Laplace Anniversary Vol-*

ume, edited by J. Neyman and L. M. LeCam (Springer-Verlag, Berlin, 1965), p. 61.
[17] C. D. Howard, Models of first passage percolation, in *Probability on Discrete Structures*, edited by H. Kesten (Springer, Berlin, 2004), pp. 125–173.
[18] A. Auffinger, M. Damron, and J. Hanson, *50 Years of FPP*, University Lecture Series Vol. 68 (American Mathematical Society, Providence, RI, 2017).
[19] M. Kardar and Y.-C. Zhang, Scaling of Directed Polymers in Random Media, Phys. Rev. Lett. **58**, 2087 (1987).
[20] J. Krug and H. Spohn, Kinetic roughening of growing surfaces, in *Solids Far from Equilibrium*, edited by C. Godrèche (Cambridge University Press, Cambridge, 1991).
[21] T. Halpin-Healy and Y.-C. Zhang, Kinetic roughening phenomena, stochastic growth, directed polymers and all that. Aspects of multidisciplinary statistical mechanics, Phys. Rep. **254**, 215 (1995).
[22] D. B. Abraham, L. Fontes, C. W. Newman, and M. S. T. Piza, Surface deconstruction and roughening in the multiziggurat model of wetting, Phys. Rev. E **52**, R1257 (1995).
[23] S. Beyme and C. Leung, A stochastic process model of the hop count distribution in wireless sensor networks, Ad Hoc Netw. **17**, 60 (2014).
[24] G. Kordzakhia and S. P. Lalley, A two-species competition model on $\mathbb{Z}^2$, Stoch. Proc. App. **115**, 781 (2005).
[25] R. Bundschuh and T. Hwa, An analytic study of the phase transition line in local sequence alignment with gaps, Discr. Appl. Math. **104**, 113 (2000).
[26] S. Chatterjee, The universal relation between scaling exponents in first-passage percolation, Ann. Math. **177**, 663 (2013).
[27] D. Richardson, Random growth in a tessellation, Proc. Cambridge Philos. Soc. **74**, 515 (1973).
[28] J. T. Cox and R. Durrett, Some limit theorems for percolation processes with necessary and sufficient conditions, Ann. Probab. **9**, 583 (1981).
[29] H. Kesten, Percolation theory and first-passage percolation, Ann. Probab. **15**, 1231 (1987).
[30] P. Córdoba-Torres, S. N. Santalla, R. Cuerno, and J. Rodríguez-Laguna, Kardar-Parisi-Zhang universality in first passage percolation: The role of geodesic degeneracy, J. Stat. Mech. (2018) 063212.
[31] D. Stauffer and A. Aharony, *An Introduction to Percolation Theory*, 2nd ed. (Taylor and Francis, Philadelphia, 2003).
[32] M. Damron, W.-K. Lam, and X. Wang, Asymptotics for 2D critical first passage percolation, Ann. Probab. **45**, 2941 (2017).
[33] M. Damron, J. Hanson, and W.-K. Lam, Universality of the time constant for 2D critical first-passage percolation, arXiv:1904.12009 [math.PR] (2019).
[34] C.-L. Yao, Law of large numbers for critical first-passage percolation on the triangular lattice, Electron. Commun. Probab. **19**, 1 (2014).
[35] C.-L. Yao, Limit theorems for critical first-passage percolation on the triangular lattice, Stoch. Proc. App. **128**, 445 (2018).
[36] H. Kesten and Y. Zhang, A central limit theorem for "critical" first-passage percolation in two dimensions, Probab. Theory Relat. **107**, 137 (1997).
[37] Y. Zhang, Supercritical behaviors in first-passage percolation, Stoch. Proc. App. **59**, 251 (1995).
[38] O. Garet and R. Marchand, Large deviations for the chemical distance in supercritical Bernoulli percolation, Ann. Probab. **35**, 833 (2007).
[39] C. Yao, A note on geodesics for supercritical continuum percolation, Stat. Prob. Lett. **83**, 797 (2013).
[40] M. Aizenman, H. Kesten, and C. Newman, Uniqueness of the infinite cluster and continuity of connectivity functions for short and long range percolation, Commun. Math. Phys. **111**, 505 (1987).
[41] H. Kesten, Aspects of first-passage percolation, in *École d'Été de Probabilités de Saint Flour XIV—1984*, Lecture Notes in Mathematics Vol. 1180, edited by R. Carmona, H. Kesten, and J. B. Walsh (Springer, Berlin, 1986), pp. 125–264.
[42] J. T. Chayes and L. Chayes, Percolation and random media, in *Critica Phenomena, Random Systems and Gauge Theories*, Les Houches Session XLIII 1984, edited by K. Osterwalder and R. Stora (North-Holland, Amsterdam, 1986), pp. 1000–1142.
[43] R. T. Smythe and J. C. Wierman, *First-Passage Percolation on the Square Lattice*, *Lecture Notes in Mathematics*, Vol. 671 (Springer, New York, 1978).
[44] A. P. Kartun-Giles, M. Barthelemy, and C. P. Dettmann, Shape of shortest paths in random spatial networks, Phys. Rev. E **100**, 032315 (2019).
[45] A. L. Ritzenberg and R. J. Cohen, First passage percolation: scaling and critical exponents, Phys. Rev. B **30**, 4038 (1984).
[46] A. R. Kerstein, Contact propagation: Percolation and other scaling regimes, Phys. Rev. B **31**, 321 (1985).
[47] A. R. Kerstein, Scaling law for the contact-propagation regime of first-passage percolation, Phys. Rev. B **31**, 7472 (1985).
[48] A. R. Kerstein and B. F. Edwards, Crossover from contact propagation to chemical propagation in first-passage percolation, Phys. Rev. B **33**, 3353 (1986).
[49] O. Garet and R. Marchand, Moderate deviations for the chemical distance in Bernoulli percolation, Alea: Lat. Am. J. Probab. Math. Stat. **7**, 171 (2010).
[50] N. Posé, K. J. Schrenk, N. A. M. Araújo, and H. J. Herrmann, Shortest path and Schramm-Loewner evolution, Sci. Rep. **4**, 5495 (2014).
[51] P. Di Francesco, P. Matthieu, and D. Sénéchal, *Conformal Field Theory* (Springer, Berlin, 1997).
[52] T. H. Cormen, C. E. Leiserson, R. L. Rivest, and C. Stein, *Introduction to Algorithms* (MIT Press, Cambridge, MA, 1990).